

COMPUTER-CONTROLLED SYSTEM FOR MEASURING TWO-DIMENSIONAL ACOUSTIC VELOCITY FIELDS

D. B. Ilić, G. S. Kino, A. R. Selfridge, and F. E. Stanke

Ginzton Laboratory
Stanford University
Stanford, CA. 94305

Abstract

An automatic system is described for measuring two-dimensional acoustic velocity fields in solid samples. The measurement is performed by a computer-controlled, mechanically-scanned transducer in a liquid bath and is based on measuring the phase delay of the acoustic wave by a two-pulse echo method. Applications include measuring stress fields due both to externally-applied and residual stresses, and microstructure studies of solid samples.

1. Introduction

Recently, there has been a resurgence of interest in studies of material properties by acoustic waves. Two important reasons for that development include the availability of dedicated computers for control of experiments and massive data processing, and the important expansion of the field of nondestructive materials evaluation (NDE). We report here on the development and the application to NDE of a measuring system which automatically produces two-dimensional images of stress distributions in metals and other solid materials.

The measuring technique is based on the two-pulse echo method developed some time ago,¹ and is applied normally to measuring propagation velocity in solid samples with bonded ultrasonic transducers.² By contrast, our experiment is carried out with a liquid buffer so that samples of a variety of shapes, sizes, and compositions can be tested by a mechanically-scanned transducer. The entire two-dimensional scanning operation is completely automated and computer-controlled, so that complete scans containing several hundred data points can be made and the results displayed in about thirty minutes. We have already reported on an early, manually-operated version of the instrument, which did not have the feature of cancelling out the water buffer propagation effects, and provided only preliminary two-dimensional scans.³ A more recent publication has reported some results of acousto-elastic measurements in metals, performed on the present system.⁴ We present here the

details of the measuring system, and then discuss some additional applications.

2. Measuring System

The measuring system consists of a liquid filled tank which is constructed as part of a mechanical rig for applying calibrated tensile or compressive loads to the plane-parallel specimen. As the acoustic wave velocity is changed by the applied stress, the variation of stress over the cross-section of a sample induced by external loading can be measured by a mechanically-scanned transducer while the load is being applied. The homemade, hydraulically-operated loading rig can apply loads up to $\sim 5 \times 10^4 \text{ N}$.

A piston transducer is scanned mechanically in the vertical and horizontal directions in the liquid-filled tank by a pair of computer-controlled stepping motors. The liquid employed is either water or ethylene glycol, the latter being more resistant to metal sample corrosion, the build-up of mineral deposits, and the occurrence of bubbles at the sample surface. Typically, an unfocused transducer is used to launch a beam of longitudinal acoustic waves of about 3 mm diameter at around 12 MHz.

The measurement principle is illustrated in Fig. 1. Two rf tone bursts a few μs long are applied to the transducer, with a variable time delay between them, Δt . The corresponding acoustic waves are launched such that they impinge on the sample at normal incidence, and longitudinal waves only are excited in the sample. At the liquid buffer/solid sample interface, the waves are partially transmitted and reflected; the reflected part propagates back and is received by the transducer, while the transmitted part of the acoustic energy undergoes further reflections at the sample back and front faces as it bounces back and forth inside the sample. Each one of these transits leads to some acoustic energy being transmitted back to the transducer, resulting in a corresponding received set of rf pulses. Because a liquid path is employed, the reflection coefficient, both at the front and the back of the sample, is not dependent on the bonding material and should be invariant with the transducer position.

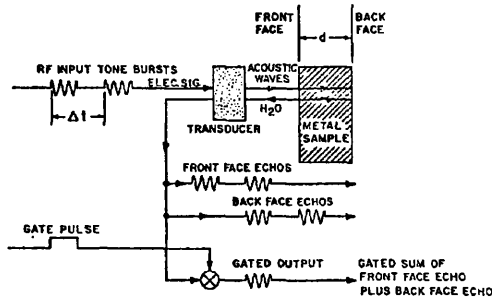


Fig. 1. The principle of the two-pulse echo measuring technique in a liquid buffer

In order to determine the local velocity of longitudinal wave propagation in the sample, Δt is adjusted so that the received rf pulses, due to the front-face echo of the second pulse and the back-face of the first pulse, overlap. This sum is then gated out from all the other received signals, and the phase shift between the two echoes is measured, corresponding to a double transit of the wave propagation through the sample. Thus, by using the front-face echo as the reference pulse, the wave propagation effects through the water buffer and the possible additional phase shifts in the outside circuitry³ are eliminated from this measurement.

3. Electronic Circuitry

3.1 Relative Velocity

The requirement for a very precise measurement of the phase difference between the front-face and the back-face echoes, which could at the same time be automated, was met by an indirect measurement, based on a nulling technique.¹ Neglecting the phase shift due to the reflection at the sample back-face, the phase change which the acoustic signal undergoes in propagating through the sample of thickness d and back again to the front face is

$$\phi = \frac{4\pi fd}{v} \quad (1)$$

where f and v are the wave frequency and velocity, respectively. For reconstructing velocity profiles in samples, we need only be concerned with velocity or transit time changes in moving from one point to the next. If we vary the carrier frequency of the rf pulses by such amounts as to keep $\phi = \text{const}$ at every point during a scan, we obtain from Eq. (1)

$$\frac{\Delta f}{f} = \frac{\Delta v}{v} - \frac{\Delta d}{d} \quad (2)$$

It has been shown that when stress is applied, both the relative change in velocity $\Delta v/v$ and the relative change in thickness $\Delta d/d$ are proportional to the applied stress.⁴ Thus, the contours of constant stress in a sample are equivalent to contours of constant frequency for which $\phi = \text{const}$. It is also seen that the constant phase shifts due to reflections drop out of this relative measurement, but are needed for an absolute measurement of velocity.

The system is required to measure the phase difference between the carriers of two coincident pulses. This could be done by varying the amplitudes of the two pulses so that they tend to cancel when they are π out of phase, but such a technique is not conven-

ient and is highly amplitude-sensitive. We therefore adopted a sampling technique in which the basic pulse repetition rate is 8 kHz but one of the pulses has its sign reversed at a 1 kHz rate. This makes it possible to use a square law detector to obtain a 1 kHz output which depends only on the product of the two pulses of interest. This product term in turn has zero amplitude when the two rf pulses have carriers $\pi/2$ out of phase with each other. A lock-in amplifier is employed to compare the 1 kHz detected signal with a 1 kHz reference so that the system can be made extremely sensitive. Furthermore, the output of the lock-in amplifier is itself employed to control a phase-lock loop, which changes the frequency of the input carrier so as to set the phase difference between the carriers of the two return pulses at $\pi/2$. Thus, the measurement system is entirely automatic.

The circuit for performing the measurement and producing results in the form of hard-copy contour plots or pictorial scan converter output is shown in Fig. 2. A free-running oscillator at 8 kHz sets the square wave pulse repetition rate and triggers the excitation of the sets of two-pulse sequences. The second pulse is further modulated by a 1 kHz signal, applied through a transistor switch (TS) in such a way that at the 8 kHz repetition rate, the square waves change sign after every four pulses. The two sets of square waves are then mixed with the output of a free-running, highly stable synthesizer (Hewlett-Packard 8660C); the resulting rf tone bursts are added, amplified by a 40 dB power amplifier and transmitted by the ultrasonic transducer.

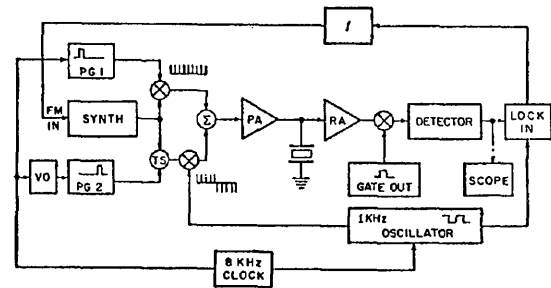


Fig. 2. Detailed block diagram of the measuring system. PG - pulse generators; VD - variable delay; PA - power amplifier; RA - limiter and receiving amplifier; SCOPE - oscilloscope monitor; LOCK-IN - lock in amplifier; SYNTH - synthesizer of rf carrier.

The received signal from the same transducer is passed through a limiter which protects the sensitive receiver from the strong transmitted signal, and then amplified by a 60 dB variable gain receiving amplifier. That signal is displayed by the oscilloscope, at which time various adjustments and calibrations are performed. Only the desired overlap of the front and back-face echoes indicated in Fig. 1 is then gated out and detected by a balanced detector (the square law detector). The signal component at 1 kHz is then synchronously detected with a lock-in amplifier with a tuned input signal channel.

In analyzing the received and gated signals, we may take the contribution from the first rf pulse signal to be of the form

$$A(t) \cos(2\pi ft + \phi) \quad (3)$$

where $A(t)$ is the pulse modulation at a repetition rate of 8 kHz. Similarly, the contribution from the second pulse, which has not propagated through the sample, has the form

$$A(t)B(t) \cos 2\pi ft, \quad (4)$$

where $B(t)$ is the 1 kHz square wave modulation of the second pulse. We note that $B(t) = \pm 1$ and that there are eight samples (pulses) per cycle of $B(t)$. If we now square the sum of Eqs. (3) and (4) and take only the contribution at 1 kHz, the corresponding input to the lock-in amplifier becomes

$$A^2 B \cos \phi. \quad (5)$$

The output is then a DC signal proportional to R , where

$$R = A^2 \cos \psi \cos \phi, \quad (6)$$

where ψ is a constant phase shift between the reference and signal paths of the 1 kHz modulating signal, and ϕ is the unknown desired phase shift.

The DC signal given by Eq. (6) is then used as an error signal in a phase-lock loop which varies the synthesizer output frequency in such a way that $R = 0$ or

$$\phi = (2n + 3)\pi/2, \quad (7)$$

since the loop locks onto every second null of $\cos \phi$. The lock-in amplifier output is first integrated (the lock-in amplifier integration constant is 1 ms, that of the integrator is 10 ms), and then applied to the FM input of the synthesizer, so that the resulting frequency f adjusts automatically to keep $R = 0$ in Eq. (6). This frequency is then read into the computer via an electronic counter, and the single-point measurement is completed.

3.2 Absolute Velocity

For performing absolute velocity measurements, the rf carrier frequency is varied over a wide range, and several neighboring nulls corresponding to Eq. (7) are recorded. We write

$$\phi_t = \frac{4\pi f_n d}{v} + \pi - \phi_d = (2n + 3)\pi/2, \quad (8)$$

where ϕ_t is the total phase shift of the back-face echo, taking into account the π shift from the sample-liquid interface, and ϕ_d is the contribution due to diffraction.⁵

An interactive computer program has been written which solves for v in two steps. First, from the slope of f_{n+k} vs. k line for several measured f_{n+k} , an approximate value of velocity v is calculated from the formula

$$v_1 = 2d(f_{n+k} - f_n)/k. \quad (9)$$

This is not accurate enough for the final calculations because it requires taking the difference of two large quantities.

The value v_1 is then used for generating the diffraction phase correction, calculated numerically for our acoustic beam diameter, sample thickness, and transducer-sample distance. Eq. (8) is next solved for n using $v = v_1$; since v_1 is used in all

these calculations instead of the unknown v , a value very close to but not exactly equal to an integer is obtained for n . That number is then rounded off to its integer value, and v is calculated from Eq. (8). An iterative scheme of several steps could also be set up, but this first iteration gives us good accuracy.

3.3 Diffraction Correction

The phase change term due to diffraction ϕ_d in Eq. (8), was derived in an approximate form, valid in the paraxial limit. The expression is very suitable for computer calculation, and the reader is referred for the derivation steps leading to it to a forthcoming publication.⁶

We are interested in the detected pressure across the face of a receiver of radius a at distance z away. The required expression is

$$\frac{\langle p_z \rangle}{\langle p_0 \rangle} = 2 \int_0^\infty e^{-j\beta z} \frac{J_1^2(\alpha a)}{\alpha} d\alpha. \quad (10)$$

Now we introduce the approximation, $k^2 \gg \alpha^2$,

$$\beta z = z \sqrt{k^2 - \alpha^2} \approx kz - \frac{\alpha^2}{2k} z, \quad (11)$$

and substituting $S = \lambda z/a^2$, where $\lambda = 2\pi/k$, $y = \alpha a$, Eq. (10) becomes

$$\frac{\langle p_z \rangle}{\langle p_0 \rangle} = 2e^{-jkz} \int_0^\infty \frac{J_1^2(y)}{y} e^{jy^2 S/4\pi} dy. \quad (12)$$

This is the final expression used in computing the phase correction due to diffraction, i.e., we take

$$\phi_d = \arg \left\{ 2 \int_0^\infty \frac{J_1^2(y)}{y} e^{jy^2 S/4\pi} dy \right\}. \quad (13)$$

This expression can be evaluated very easily on the computer, and that is what we do in performing the absolute velocity measurements. As an illustration, the results of calculating Eq. (13) are plotted in Fig. 3, both for the phase and the attenuation corrections (the latter is important for correcting attenuation measurements). These results agree well with the more elaborate calculations reported in the literature.^{5,7}

4. Measuring Procedure and Computer Interfacing

Initial calibration consists of mechanically aligning the transducer with respect to the sample for maximum front-face reflection, and then adjusting separately the pulse widths of PG1 and PG2 (refer to Fig. 2) such that echoes from one pulse do not overlap, depending on sample thickness and velocity of propagation. For typical samples of 1 cm thick aluminum or steel, the required pulse widths range from 1 to several μs . Next, the delay of the second pulse (VD) is adjusted for total overlap of the front-face echo of the second pulse with the back-face echo of the first pulse (a few μs), and the attenuation (VA) adjusted for the two pulses to have about equal amplitudes. Finally, the delay of the gating signal and the appropriate pulse width of are adjusted to pick out the desired sum, and the center frequency and the FM level of the synthesizer are adjusted for appropriate excursions for proper frequency null

tracking. Typically, for the above stated conditions, the FM level is ~50 kHz, where $\Delta f \sim 300$ kHz corresponds to $\Delta\phi = 2\pi$ at $f \sim 12$ MHz. The measurement precision routinely corresponds to $\Delta v/v$ of about 10^{-6} with metal samples of the order of 1 cm thick. This is about the same or better than that obtained in the non-scanned, bonded transducer experiments based on pulse superposition, or sing-around methods.²

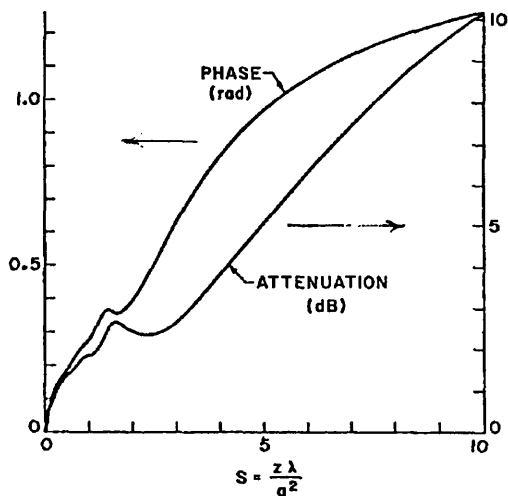


Fig. 3. Computed diffraction corrections to phase and amplitude

The measuring procedure for scanning a sample involves defining the grid of transducer positions in computer software, and after the initial sample and transducer alignment and electronics calibration, a corresponding array of frequency values of nulls of Eq. (6) is generated under complete computer control, at the rate of a few seconds per point. The data points are displayed either as contour plots of equal velocities or as equivalent scan converter output.⁴

5. Applications

The system we have described is routinely used by a varied group of electrical and mechanical engineers and materials scientists. We have already reported some exciting measurements of third order elastic constants and comparisons between measured and calculated stress fields in externally-loaded samples of different shapes.⁴ Such contour plots can also give us very useful qualitative information about stresses around cracks and can be used to evaluate crack stress intensity factors. More recent work has included similar measurements of residual stress fields in samples with stresses built into them by a process of hydrostatic extrusion. Absolute values of radial and hoop stresses can then be obtained by suitable integration of contour data. We are just at the beginning of these latter, quantitative applications, and the prospects for NDE are exciting indeed.

We present here a recent example of the application of this system to the study of a standard end-quench Jominy bar, which is a steel rod with a widely varying hardness along its axis. The rod is normally used as a standard for measuring the hardening response to heat treatment of steel samples. It is prepared by introducing a temperature gradient along the bar axis, so that the resultant gradient in cooling rate causes a marked gradation in steel microstructure and consequently hardness. Fig. 4 shows the results of hardness (Rockwell C) measurements together with a one-

dimensional acoustic velocity scan, showing strong correlation between the two curves. It is seen that the velocity of propagation decreases as hardness is increased.

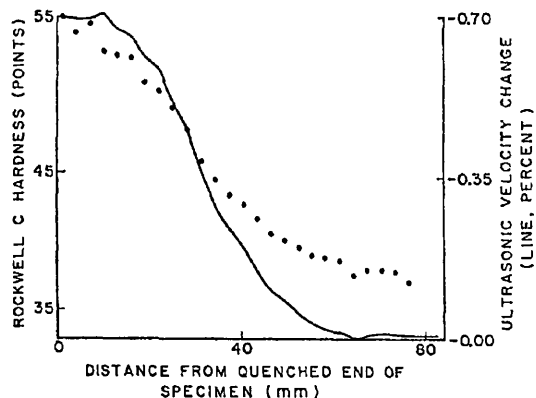


Fig. 4. Spatial dependences of Rockwell C hardness (points) and ultrasonic velocity (line) of an end-quench Jominy bar of AISI 4140 steel. $v = 5.9$ km/s

Absolute velocity measurements are also being carried out with this system, as described in the previous section. This method is not as accurate as the relative measurement described, because measurements over a wide range of frequencies must be made, and extraneous factors such as diffraction corrections, amounting to about 0.15% in our case, should be taken into account.² We are also limited by the thickness accuracy of our samples to about $2 \mu\text{m}$ on 1 cm samples, which limits the ultimate total accuracy to about 2×10^{-4} . This is consistent with the general statement that the precision of relative velocity scans is about two orders of magnitude better than the accuracy of absolute velocity measurements.² However, if thickness could be measured accurately, the precision of the absolute velocity measurement would be improved accordingly.

Finally, we are now preparing a shear wave scanner with specially constructed contact transducers to be used in conjunction with this system. Shear wave data will enable us to get the values of both principal stresses individually, by rotating the transducer with respect to the axis of preferred orientation, instead of just the sum of the principal stresses produced by the above longitudinal wave data.⁴

This work was supported by EPRI under Contract RP 609-1, NSF Contract DMK-76-00726 through the Center for Materials Research at Stanford University, and by Air Force Office of Scientific Research Grant 78-3726.

References

1. H. J. McSkimin, *J. Acous. Soc. Am.*, **37**, 864 (1965).
2. E. P. Papadakis in *Physical Acoustics: Principles and Methods*, W. P. Mason and R. N. Thurston, eds., vol. XII, pp. 277-323 (1976).
3. J. Souquet and G. S. Kino, *J. Appl. Phys.*, **47**, 5482 (1976).
4. G. S. Kino, J. B. Hunter, G. C. Johnson, A. R. Selfridge, D. M. Barnett, G. Herrmann, and C. R. Steele, *J. Appl. Phys.*, **50**, 2607 (1979).
5. E. P. Papadakis in *Physical Acoustics: Principles and Methods*, W. P. Mason and R. N. Thurston, eds., vol. XI, pp. 151-211 (1975).
6. D. B. Ilic, G. S. Kino, and A. R. Selfridge, *Rev. Sci. Instrum.* (in press).
7. G. C. Benson and O. Kiyohara, *J. Acous. Soc. Am.*, **55**, 184 (1974).